# Synthesis of Exotic Zigzag ZnO Nanoribbons and Their Optical, Electrical Properties

**Li Wang,[†] Kezheng Chen,*[,†] and Lifeng Dong[†,‡]**

*College of Materials Science and Engineering, Qingdao University of Science and Technology, Qingdao 266042, People's Republic of China, and Department of Physics, Astronomy, and Materials Science, Missouri State University, Springfield, Missouri 65810, United States*

*Received: May 22, 2010; Revised Manuscript Received: August 22, 2010*

ZnO nanoribbons with zigzag edges and ultrafine nanowire-like tips (diameter about 10 nm) were synthesized via a facile method at a relatively low temperature without any catalysts or templates. The nanoribbons are about 30 nm in thickness, 500 nm in length, and tapered in width. It is hydrogen peroxide that results in the formation of ZnO nanoribbons with zigzag edges. As an oxidant, hydrogen peroxide provides not only oxygen for the growth of ZnO nanoribbons but also water vapor for impeding the growth of the nanoribbons along [0001] and accelerating the $<01\bar{1}0>$ growth of ZnO nanoribbons. Bottom-gate ZnO-nanoribbon-based field-effect transistors demonstrated n-type field-effect conduction, and the current on-to-off ratio was as high as $1 \times 10^4$. The novel method developed in this study can be used to synthesize other metal oxides with zigzag edges.

## Introduction

In recent years, extensive theoretical and experimental research on ZnO nanostructures has been triggered by their potential application as building blocks for optoelectronic devices, sensors, field emission devices, and electrochromic displays.[1−6] Much work has been spent on selecting a desired synthesis method and controlling experimental parameters to obtain ZnO nanostructures with various and controllable morphologies. Metal−organic vapor-phase epitaxial growth, chemical vapor deposition, thermal evaporation, electrochemical deposition, and lithographic techniques have been used to synthesize various types of ZnO nanostructures, such as multipeds; nanorods; nanonails; and tower-like, comblike, and hierarchical structures.[7−13] Among those nanostructures, one-dimensional (1D) structures are regarded as an ideal system for understanding their unique optical, thermal, and electrical properties.[14] ZnO nanowires/nanobelts, along with carbon nanotubes and silicon nanowires, are considered the most important 1D nanomaterials as building blocks for nanoscale devices.[15]

Patterned and aligned nanowires (NWs) can be obtained by patterning catalytic particles, and the diameters of the nanowires can be controlled by the size of catalyst particles.[16] Without catalysts, the majority of NWs were greater than 50 nm in size, and the NWs had hexagonal cross sections.[17,18] Recently, zigzag graphene nanoribbons have sparked significant interest toward zigzag nanostructures.[19,20] For instance, zigzag-shaped nanostructures of $SnO_2$ and $TiO_x$ and other semiconductors have been reported.[21−23] Theoretical research on peculiar magnetic states at the edges of a zigzag ZnO nanoribbon has also encouraged the study of ZnO nanoribbons with different layers.[24]

By far, 1D semiconductor NWs have been synthesized using chemical vapor deposition (CVD).[25] Experimental results demonstrated that a high temperature (>1000 °C) is required for the CVD growth of ZnO nanowires while using ZnO powder as a precursor. Even via a carbothermal reduction of ZnO powder, the reaction temperature is still as high as 800−900 °C.[26] Besides growth temperatures, the CVD growth method also needs other controllable parameters, such as vacuum pressure, gas composition, and gas flow rates. Recent studies indicate that oxygen vacancies during the CVD process might produce active sites, and the active sites advance gas absorption of carbon dioxide, ethanol, methanol, and water molecules on nanowire surfaces[27,28] in addition to active sites. Water vapor enhanced the crystallization of ZnO nanostructures. Inspired by these reports, we developed a two-step method using hydrogen peroxide ($H_2O_2$) as an oxygen source to synthesize zigzag ZnO nanostructures with exotic morphologies and investigated their optical and electrical properties.

## Experimental Section

The synthesis of ZnO nanostructures consists of two steps: thermal evaporation of zinc powder and the growth of ZnO nanostructures under a $H_2O_2$ atmosphere. Both processes are carried out in a horizontal quartz tube furnace.

**Thermal Evaporation of Zinc Powder.** Metallic zinc powder (purity of 99.98%) was used as a source material to form a zinc seed film. A 1.0 g portion of zinc powder was loaded in a ceramic boat at the center of the furnace. Glass slices or silicon substrates were put in the quartz tube along the downstream side of the flowing nitrogen with an approximate distance of 110 mm to the center of the furnace. Prior to evaporation, high-purity nitrogen, used as a protective and carrier gas, was introduced into the quartz tube for 30 min to remove oxygen inside. The furnace was heated to 550 °C with a heating rate of 10 °C/min, held at 550 °C for 30 min, and then cooled to room temperature under a nitrogen flow.

**Growth of ZnO Nanostructures.** Glass or silicon substrates coated with a zinc film were put in the middle of the furnace, and then a ceramic boat filled with 4 mL of 30% $H_2O_2$ and 6 mL of distilled water was located at a region that is about 10 cm away from the substrates. To avoid the introduction of impurities, the tube furnace was sealed and vacuumed. The tube was heated to 500 °C from room temperature with a heating rate of 10 °C/min, held for 30 min, and then cooled to room

* To whom correspondence should be addressed. Tel: 86-532-84022509. Fax: 86-532-84022509. E-mail: kchen@qust.edu.cn.
† Qingdao University of Science and Technology.
‡ Missouri State University.

10.1021/jp104706q 
Published on Web 09/28/2010

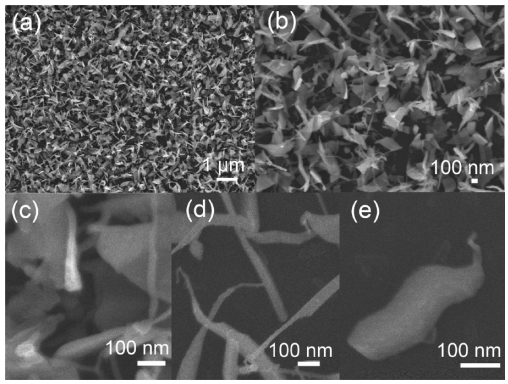


**Figure 1.** SEM images of zigzag ZnO nanoribbons with different magnifications.

temperature. After the growth procedure, the substrates were coated with white ZnO nanostructures. A number of experiments were conducted with substrates located in different zones and in different atmospheres, such as in an air condition and water vapor.

**Structural Characterizations and Electrical/Optical Measurements.** The morphology and crystal structure of as-grown product were characterized with field emission scanning electron microscopy (FESEM, JEOL JSM-6700F) and transmission electron microscopy (TEM, JEOL JEM-2100F). The X-ray diffraction (XRD) data were collected on a D-MAX 2500/PC diffractometer. The photoluminescence (PL) measurements were performed on a Jobin Yvon LabRAM HR 800UV micro-Raman/PL system with an Andor DU420 classic CCD detector under the excitation of a He−Cd laser (325 nm). Bottom-gate ZnO nanostructure-based field-effect transistors (FETs) were fabricated by utilizing a highly doped Si substrate as a gate electrode and $SiO_2$ with a thickness of 200 nm as a gate dielectric. First, gold electrodes were deposited by a photolithography technique. The channel width ($W$) and length ($L$) were 2000 and 50 $\mu$m, respectively. ZnO nanoribbons were then synthesized by the evaporation and thermal oxidation process on silicon substrates with the patterned gold electrodes. FET characteristics were measured using a Keithley SCS 4200 semiconductor characterization system.

## Results and Discussion

As shown in Figure 1a,b, the substrate is covered with a large quantity of ZnO nanoribbons. The morphologies of the ribbons are uniform, with a thickness of 20 nm and length up to hundreds of nanometers; moreover, the width is tapered along the growth direction (Figure 1c−e). Figure 1d demonstrates ultrafine tips with a diameter of ~10 nm on each nanoribbon. Figure 1e shows a zigzag edge of the ribbon, which has been rarely reported up to now. Each nanostructure can be considered as a combination of a nanoribbon with a zigzag edge and a nanowire. A nanostructure of this type may exhibit unique current−voltage ($I-V$) characteristics for nanoelectronics.[29] To understand the effect of $H_2O_2$ on the growth of zigzag structures, various experiments were performed in different atmospheres by keeping all other reaction parameters the same. As given in Figure 2, when water vapor or air was introduced instead of $H_2O_2$, flexuous wires and nanorods were obtained, respectively. The wires with rough surfaces (Figure 2a) are up to micrometers in length and submicrometers in diameter, which might be Zn/Zn suboxide; there are also some seedlike nanocrystals on the substrate (Figure S1, Supporting Information). The nanorods obtained in the air condition (Figure 2b) have a uniform diameter of about 100 nm. The XRD pattern (Figure S2, Supporting Information) demonstrates that the nanorods are wurtzite hexagonal phase ZnO (JCPDS 36-1451) and grow along the [0001] direction, which is consistent with other reports.[30] 1D nanostructures of zinc oxide are usually formed by one of the following two processes: the vapor−liquid−solid (VLS) mechanism or the vapor−solid (VS) mechanism.[31] Metal catalysts were not used or detected, and thereby, the reaction in our experiment cannot be attributed to the VLS process. Though the VS mechanism is frequently cited for the formation of ZnO nanostructures, it is not suitable for our two-step process due to the low temperature. We proposed that the zinc seed film was first oxidized to form zinc oxides on the surface. Zinc atoms then diffuse into $ZnO_x$ and induce the growth of 1D nanostructures through the migration of intrinsic defects.[32] The selection of oxidant and the diffusion rate of zinc are two dominating factors for the morphology of the nanostructures. Figures 1 and 2 demonstrate that $H_2O_2$ plays a crucial role in the formation of exotic ZnO nanoribbons, and an oxidant can be used to tailor the growth of ZnO nanostructures with desired morphologies.

Internal structures of the nanoribbons were studied through TEM characterizations. Figure 3a shows the basal portion of a nanoribbon (the nanowire on the tip was broken during the ultrasonic process for the TEM sample preparation), which is consistent with SEM observations. The typical zigzag shape is more clearly shown through TEM imaging. Planes of $(01\bar{1}1)$, $(01\bar{1}2)$, and $(01\bar{1}3)$ are designated by different colored arrows (black, red, and blue, respectively). A selected area electron diffraction (SAED) pattern with the incident electron beam along $[2\bar{1}\bar{1}0]$ reveals that the top and bottom planes are $(2\bar{1}\bar{1}0)$ and the growth orientations are along [0001] and $[01\bar{1}0]$, which correspond to three favored growth directions of wurtzite-structured oxide, [0001], $<01\bar{1}0>$, and $<2\bar{1}\bar{1}0>$.[33] On the basis of the experimental results above and in combination with the crystal structure of wurtzite (Figure 3b), we propose that zigzag-shaped nanoribbons are surrounded by (0002), $(01\bar{1}0)$, $(01\bar{1}1)$, $(01\bar{1}2)$, and $(01\bar{1}3)$ and with $(2\bar{1}\bar{1}0)$ as the top and bottom planes.

As a polar crystal, Zn and O atoms arrange alternatively along the $c$ axis.[34] ZnO 1D nanostructures mostly grow along [0001] and have a hexagonal cross section. For zigzag ZnO nanostructures here, the tapered width indicates different growth rates along two directions owing to the effect of water vapor during the growth process. Similar structures, such as Sb-doped ZnO nanobelts with single-sided zigzag boundaries, were achieved by Zhang et al.[35] They found that a certain concentration of Sb element results in the formation of a single-sided zigzag shape. In our case, without other elements, hydrogen peroxide decomposed at a low temperature and released oxygen for the growth of ZnO nanostructures. Both $Zn^{2+}$ and $O^{2-}$ tend to absorb $H_2O$ molecules. $H_2O$ has been reported to have effects on impeding the growth along [0001] and accelerating the $<01\bar{1}0>$ growth of ZnO.[36,37] Though growth kinetics need to be further investigated, the formation of ZnO nanostructures indicates the important role of the hydrogen peroxide.

The surfaces of the ribbons are not as smooth as those of the 1D nanostructure prepared by the CVD method. There are nanoislands on both the top/bottom plane and edges with diameters of approximately 30 nm, as shown in Figure 4. This growth phenomenon could be due to absorption and self-attraction of ZnO crystals.[38] These islands increase the surface area, thereby improving their functions as catalysts and sensors.

To investigate optical properties of the nanostructures, photoluminescence (PL) spectra were measured with an excitation wavelength of 325 nm at room temperature. As presented

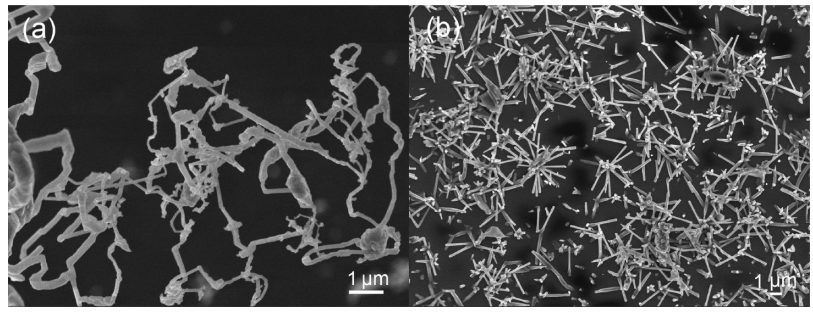


**Figure 2.** SEM images of ZnO nanostructures obtained in (a) a water vapor condition and (b) an air condition.

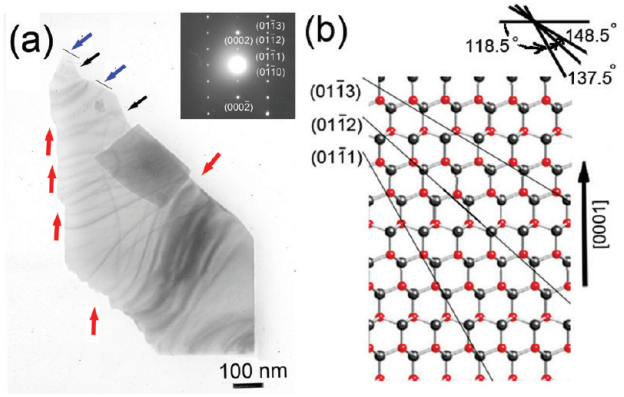


**Figure 3.** (a) TEM image and SAED pattern of a typical zigzag ribbon with the incident electron beam along [2$\bar{1}\bar{1}$0]. (b) Structural model of wurtzite-structured ZnO with (01$\bar{1}$1), (01$\bar{1}$2), and (01$\bar{1}$3) planes labeled.

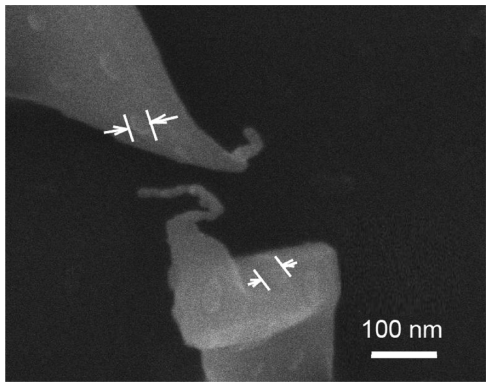


**Figure 4.** SEM image of ZnO nanostructures.

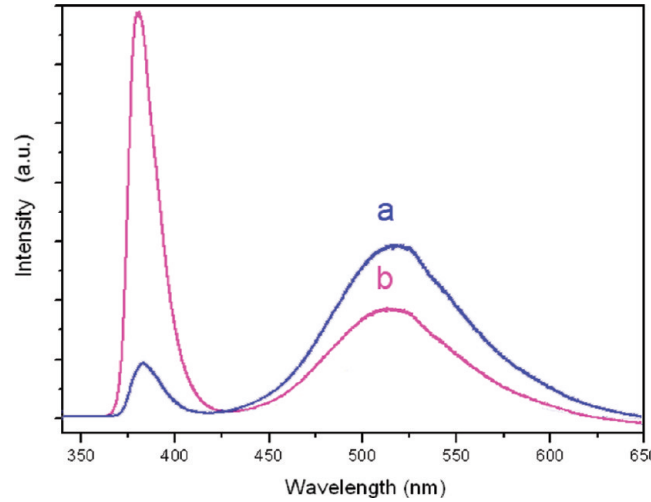


**Figure 5.** Photoluminescence spectra of (a) nanowire-like ZnO nanostructures and (b) zigzag ZnO nanostructures.

in Figure 5, there are mainly two emission peaks for ZnO nanostructures with an ultraviolet (UV) emission at about 382 nm and a green peak at 518 nm. The UV peak could be generally attributed to the near-band-edge emission (NBE) and the visible band (known as deep level emission, DLE) is usually caused by impurities and structural defects.[39] In comparison to nanowire-like structures formed at a lower temperature zone, the intensity of the UV emission of zigzag ZnO nanostructures increases dramatically, and the intensity of visible emission obviously decreases. The nanowire-like structures were obtained as the substrate was located about 13 cm away from the center of the furnace (Figure S3, Supporting Information). The intensity ratios of the UV emission to the visible emission of the zigzag and nanowire-like nanostructures are 3.73 and 0.31, respectively. A higher ratio indicates an improved crystallinity of the zigzag ZnO nanostructures and few ionized oxygen vacancies inside.[40]

Bottom-gate ZnO FETs were constructed on a $Si/SiO_2$ substrate using $P^{++}-Si$, $SiO_2$, and Au as the gate electrode, gate dielectric, and source/drain electrodes, respectively (inset of Figure 6a). The thickness of the ZnO semiconductor is about 100 nm. Typical $I_d-V_{ds}$ curves of the device fabricated in this manner are shown in Figure 6a. ZnO FETs demonstrated characteristics of a conventional transistor in both linear and saturation regimes with $I_{ds}$ increasing linearly with $V_{ds}$ at low drain voltages and saturation behavior at high drain voltages. As shown in Figure 6b, ZnO nanostructures exhibit a typical n-channel behavior with a threshold voltage ($V_{th}$) of 16 V. The saturation mobility and current on-to-off ratio from the transfer plot at a drain voltage ($V_{ds}$) of 20 V and gate voltages ($V_g$) of $-10$ to 40 V were 0.063 $cm^2\ V^{-1}\ s^{-1}$ and $1 \times 10^4$, respectively. The electron mobility and threshold voltage are obtained from the following equation

$$I_{ds} = \left(\frac{C_i \mu_{sat} W}{2L}\right)(V_{gs} - V_{th})^2$$

where $C_i$ is the capacitance per unit area of the gate insulator ($C_i = 17.1$ nF $cm^{-2}$). The low mobility can be related to high contact resistance between ZnO nanoribbons and electrodes.[41,42] In comparison to ZnO films prepared by sputtering coating or spin-coating, the film used in this study consists of a large number of ZnO nanoribbons that could make a film of ZnO nanoribbions a promising material for applications in catalysts and sensors due to its large specific surface area. Low-temperature processing makes the fabrication of such a ZnO film on an indium tin oxide (ITO) substrate practical. Like ZnO nanorod arrays, ZnO nanoribbons will also become a very promising material as an electron-transport layer in dye-sensitized solar cells.

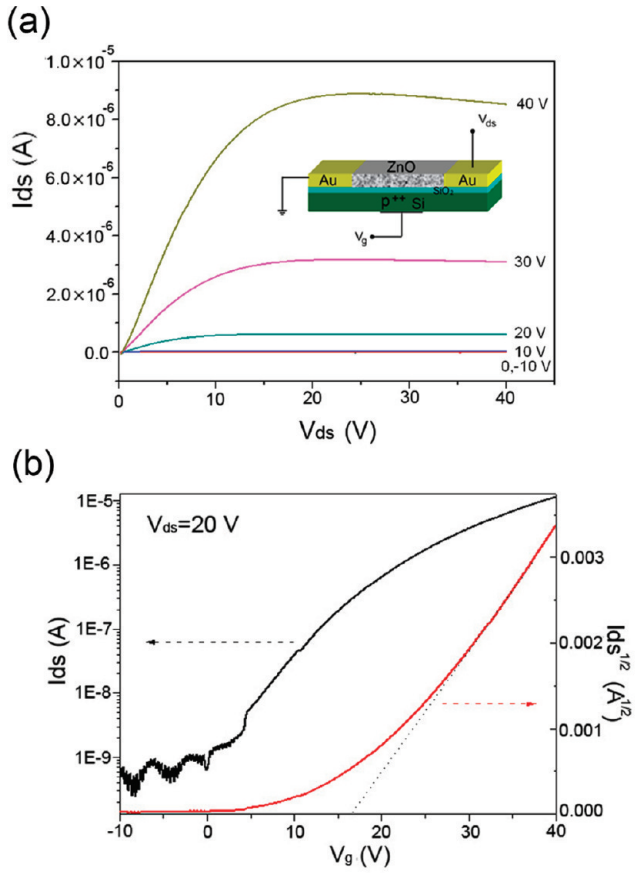


**Figure 6.** (a) Output characteristics and (b) transfer characteristics of a ZnO-nanoribbon-based field-effect transistor.

## Conclusion

A novel method was investigated to synthesize exotic zigzag ZnO nanostructures at a low temperature of 500 °C with the aid of hydrogen peroxide as an oxidant. Such a low growth temperature is compatible with very developed silicon technology. SEM and TEM characterizations show that the nanostructures are a single crystal with a thickness of 20 nm, a length up to hundreds of nanometers, and a width tapered along the growth direction. Optical and electrical measurements demonstrate that zigzag ZnO nanostructures should be a promising material for nanoscale optoelectronics, field-effect transistors, and solar cells. The novel method developed in this study can be used to synthesize other metal oxides with zigzag edges.

**Acknowledgment.** This work was financially supported by the Natural Science Foundation of Shandong Province (Grant No. 2009ZRB01420). L.F.D. acknowledges financial support by the Taishan Scholar Overseas Distinguished Professorship program from the Shandong Province Government, People's Republic of China.

**Supporting Information Available:** SEM images and XRD pattern of ZnO nanostructures. This material is available free of charge via the Internet at http://pubs.acs.org.

## References and Notes

(1) Sun, X. W.; Huang, J. Z.; Wang, J. X.; Xu, Z. *Nano Lett.* **2008**, *8*, 1219–1223.
(2) Kwon, S. S.; Hong, W. K.; Jo, G.; Maeng, J.; Kim, T. W.; Song, S.; Lee, T. *Adv. Mater.* **2008**, *20*, 4557–4562.
(3) Cao, X.; Wang, N.; Wang, L. *Nanotechnology* **2010**, *21*, 065603.
(4) Jang, E. S.; Won, J. H.; Hwang, S. J.; Choy, J. H. *Adv. Mater.* **2006**, *18*, 3309–3312.
(5) Zhou, J.; Gu, Y. D.; Fei, P.; Mai, W. J.; Gao, Y. F.; Yang, R.; Bao, G.; Wang, Z. L. *Nano Lett.* **2008**, *8*, 3035–3040.
(6) Jun, J. H.; Park, B.; Cho, K.; Kim, S. *Nanotechnology* **2009**, *20*, 505201.
(7) Fragala, M. E.; Satrianob, C.; Malandrinoa, G. *Chem. Commun.* **2009**, 839–841.
(8) Bacsa, R. R.; Dexpert-Ghys, J.; Verelst, M.; Falqui, A.; Machado, B.; Bacsa, W. S.; Chen, P.; Zakeeruddin, S. M.; Graetzel, M.; Serp, P. *Adv. Funct. Mater.* **2009**, *19*, 875–886.
(9) Wang, X. Y.; Tian, Z. P.; Yu, T.; Tian, H. M.; Zhang, J. Y.; Yuan, S. K.; Zhang, X. B.; Li, Z. S.; Zou, Z. G. *Nanotechnology* **2010**, *21*, 065703.
(10) Cao, B. Q.; Cai, W. P.; Duan, G. T.; Li, Y.; Zhao, Q.; Yu, D. P. *Nanotechnology* **2005**, *16*, 2567–2574.
(11) Hu, P. A.; Liu, Y. Q.; Wang, X. B.; Fu, L.; Zhu, D. B. *Chem. Commun.* **2003**, 1304–1305.
(12) Pan, Z. W.; Mahurin, S. M.; Dai, S.; Lowndes, D. H. *Nano Lett.* **2005**, *5*, 723–727.
(13) Chou, T. P.; Zhang, Q. F.; Fryxell, G. E.; Cao, G. Z. *Adv. Mater.* **2007**, *19*, 2588–2592.
(14) Sun, T. J.; Qiu, J. S.; Liang, C. H. *J. Phys. Chem. C* **2008**, *112*, 715–721.
(15) Wang, Z. L. *ACS Nano* **2008**, *2*, 1987–1992.
(16) Wang, N.; Cai, Y.; Zhang, R. Q. *Mater. Sci. Eng., R* **2008**, *60*, 1–51.
(17) Umar, A.; Karunagaran, B.; Kim, S. H.; Suh, E. K.; Hahn, Y. B. *Inorg. Chem.* **2008**, *47*, 4088–4094.
(18) Chen, L. Y.; Wu, S. H.; Yin, Y. T. *J. Phys. Chem. C* **2009**, *113*, 21572–21576.
(19) Zhang, Z. H.; Guo, W. L. *Appl. Phys. Lett.* **2009**, *95*, 023107.
(20) Kan, E. J.; Li, Z. Y.; Yang, J. L.; Hou, J. G. *J. Am. Chem. Soc.* **2008**, *130*, 4224–4225.
(21) Duan, J. H.; Yang, S. G.; Liu, H. W.; Gong, J. F.; Huang, H. B.; Zhao, X. N.; Zhang, R.; Du, Y. W. *J. Am. Chem. Soc.* **2005**, *127*, 6180–6186.
(22) Barcaro, G.; Sedona, F.; Fortunelli, A.; Granozzi, G. *J. Phys. Chem. C* **2007**, *111*, 6095–6102.
(23) Lou, P.; Lee, J. Y. *J. Phys. Chem. C* **2009**, *113*, 21213–21217.
(24) Botello-Mendez, A. R.; Lopez-Urias, F.; Terrones, M.; Terrones, H. *Nano Lett.* **2008**, *8*, 1562–1565.
(25) Wei, D. P.; Ma, Y.; Pan, H. Y.; Chen, Q. *J. Phys. Chem. C* **2008**, *112*, 8594–8599.
(26) Kuo, T. J.; Lin, C. N.; Kuo, C. L.; Huang, M. H. *Chem. Mater.* **2007**, *19*, 5143–5147.
(27) Sun, S. H.; Meng, G. W.; Zhang, G. X.; Zhang, L. D. *Cryst. Growth Des.* **2007**, *7*, 1988–1991.
(28) Zhang, Y.; Xu, J. Q.; Xiang, Q.; Li, H.; Pan, Q. Y.; Xu, P. C. *J. Phys. Chem. C* **2009**, *113*, 3430–3435.
(29) Zhan, J. H.; Bando, Y.; Hu, J. Q.; Golberg, D.; Kurashima, K. *Small* **2006**, *2*, 62–65.
(30) Liu, F.; Cao, P. J.; Zhang, H. R.; Shen, C. M.; Wang, Z.; Li, J. Q.; Gao, H. J. *J. Cryst. Growth* **2005**, *274*, 126–131.
(31) Kar, S.; Pal, B. N.; Chaudhuri, S.; Chakravorty, D. *J. Phys. Chem. B* **2006**, *110*, 4605–4611.
(32) Danielewski, M.; Filipek, R.; Kozubski, R.; Kucza, W.; Zieba, P.; Zurek, Z. *Diffus. Defect Data, Pt. A* **2005**, *237−240*, 163–168.
(33) He, J. H.; Ho, C. H.; Wang, C. W.; Ding, Y.; Chen, L. J.; Wang, Z. L. *Cryst. Growth Des.* **2009**, *9*, 17–19.
(34) Shen, J. B.; Zhuang, H. Z.; Wang, D. X.; Xue, C. S.; Liu, H. *Cryst. Growth Des.* **2009**, *9*, 2187–2190.
(35) Yang, Y.; Qi, J. J.; Liao, Q. L.; Zhang, Y.; Tang, L. D.; Qin, Z. *J. Phys. Chem. C* **2008**, *112*, 17916–17919.
(36) Ali, M.; Winterer, M. *Chem. Mater.* **2010**, *22*, 85–91.
(37) Wang, H. H.; Xie, C. S.; Zeng, D. W. *J. Cryst. Growth* **2005**, *277*, 372–377.
(38) Han, X. H.; Wang, G. Z.; Zhou, L.; Hou, J. G. *Chem. Commun.* **2006**, 212–214.
(39) Khranovskyy, V.; Yazdi, G. R.; Lashkarev, G.; Ulyashin, A.; Yakimova, R. *Phys. Status Solidi A* **2008**, *205*, 144–149.
(40) Liu, Y. C.; Xu, H. Y.; Mu, R.; Henderson, D. O.; Lu, Y. M.; Zhang, J. Y.; Shen, D. Z.; Fan, X. W.; White, C. W. *Appl. Phys. Lett.* **2003**, *83*, 1210–1212.
(41) Schneider, J. J.; Hoffmann, R. C.; Engstler, J.; Soffke, O.; Jaegermann, W.; Issanin, A.; Klyszcz, A. *Adv. Mater.* **2008**, *20*, 3383–3387.
(42) Choi, J. H.; Kar, J. P.; Khang, D. Y.; Myoung, J. M. *J. Phys. Chem. C* **2009**, *113*, 5010–5013.

JP104706Q